Locking of commensurate phases in the planar model in an external magnetic field

A. B. Harris
Department of Physics, University of Pennsylvania, Philadelphia, Pennsylvania 19104

E. Rastelli and A. Tassi
Dipartimento di Fisica dell'Universitá, 43100 Parma, Italy
(Received 30 January 1991)

Commensurate configuration locking is known in models like the anisotropic next-nearest-neighbor Ising model and the Frenkel-Kontorova model. We find an analogous scenario in the planar model with competing interactions when an external magnetic field is applied in the plane in which the spins lie. This model falls in the same symmetry class of the Heisenberg model with planar anisotropy. We performed a low-field, low-temperature expansion for the free energy of the model and we find phase locking energy for states with wave vectors of the form $\mathbf{G}/p$ where p is an integer and $\mathbf{G}$ is a reciprocal-lattice vector. The helix characterized by $p=3$ is peculiar because the commensuration energy vanishes at zero temperature. The helix corresponding to $p=4$ is not stable against the switching of a magnetic field that forces the spins into an up-up-down-down configuration analogous to the spin-flop phase of an antiferromagnet. For a generic commensurate value of $p>4$, we expect locking both at zero and finite temperature as we have verified for $p=5$ and 6. The consequences of our results are examined for the $3N$ model (a tetragonal spin lattice with in-plane competitive interactions up to third-nearest neighbors).

I. INTRODUCTION

Helical magnetic systems (helimagnets) give rise to a number of interesting phenomena. In this paper we will mainly be concerned with a calculation of the pinning potential which gives rise to commensurate states when a helimagnet is subject to a uniform applied magnetic field orientated in the plane of polarization of the spins. For definiteness we consider continuous spin systems with (a) a strong easy-plane anisotropy, (b) a uniform applied magnetic field H oriented within the easy plane, and (c) competing exchange interactions such that the zero-temperature ordered phase for $H=0$ is a magnetic helix. The relevant Hamiltonian is

$$\mathcal{H}=-\sum_{i,j} J_{ij}\cos(\phi_i-\phi_j)-H\sum_i \cos\phi_i \ , \tag{1.1}$$

where ϕ_i is the angle the ith spin makes with the magnetic field. The phase diagram for the model of Eq. (1.1) for $H=0$ is shown in Fig. 1.

The system described by Eq. (1.1) was studied by Nagamiya, Nagata, and Kitano[1,2] on the basis of low- and high-field series expansions. They concluded that there existed a low-field phase characterized by a continuously distorted helix in which all orientations ϕ_i occur with nonzero frequency and a high-field "fan" phase where spin orientations opposite to the field do not occur. It was argued[1,2] that at intermediate fields there would be a first-order helix-fan phase transition. This picture was in accord with the idea[3,4] that the elementary excitation spectrum does not have a gap at zero wave vector $\mathbf{k}$. The absence of such a gap is found within simple spin-wave theory and is also the result of an adapted nonrelativistic Goldstone theorem.[3] However, in general, the hypothesis on which this theorem is based is false, as we shall demonstrate because the ground state of a commensurate helix in presence of magnetic field is unique, so that the adapted Goldstone theorem[3] cannot be invoked.

In this paper, indeed, we perform an exact low-temperature, low-field expansion of the free energy for a classical planar model and we have proven that commensurate helices are locked by the magnetic field, the commensuration energy being of order $(\mu H/2J_1)^p$, where μ is the magnetic moment localized on a lattice site, H is the external magnetic field, $2J_1$ is the nearest-neighbor (NN) exchange interaction, and p is the number of spins in a unit magnetic cell. For arbitrary p one finds commensuration energy both for zero and finite temperature, but for $p=3$ the commensuration energy shows accidental vanishing at zero temperature. Preliminary results[5] of these calculations were presented at the Conference on Magnetism and Magnetic Materials (Boston, 1989). In a future paper[6] we will show that the accidental vanishing of the commensuration energy at $T=0$ for $p=3$ is removed by quantum fluctuations.

The case characterized by $p=4$ spins for cell is anomalous with respect to the traditional expectation of distorted helix. Indeed, we find that the helix with $\mathbf{Q}=\mathbf{G}/4$, where $\mathbf{G}$ is a reciprocal lattice vector, is not stable against the switching of a magnetic field. We have found that stable configurations are somewhat similar to the spin-flop phase of an antiferromagnet. These configurations consist on "up-up-down-down" patterns where the spins are nearly perpendicular to the magnetic field. Such a configuration evolves continuously into a paramagnetic-saturated configuration as the magnetic field is increased sufficiently. Although we do not give any calculations of the pinning energy, it seems clear that

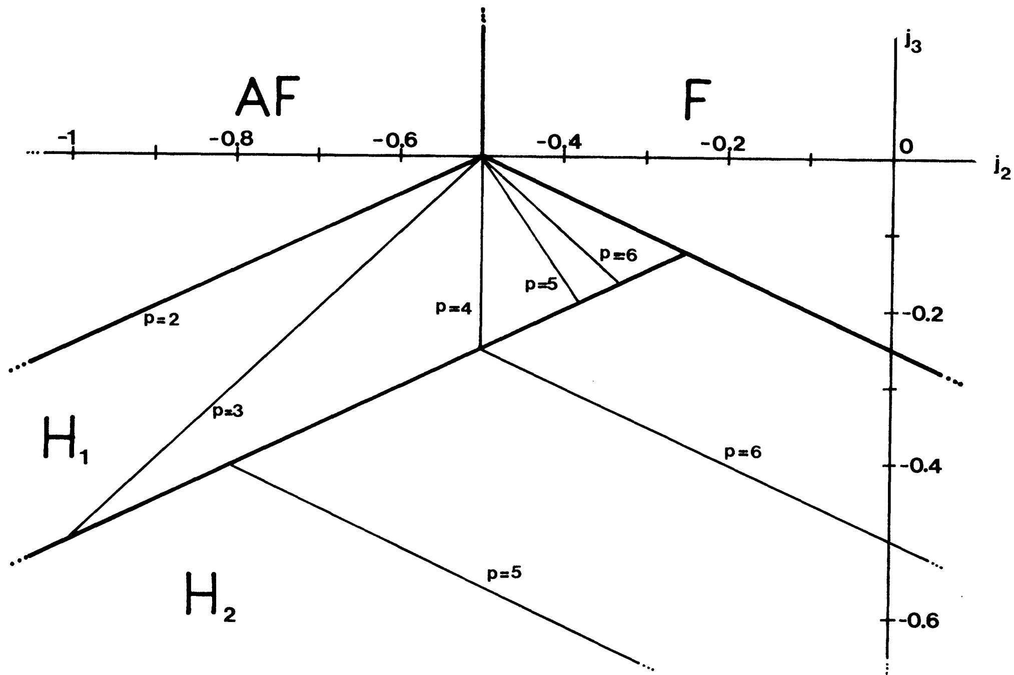

FIG. 1. Zero-temperature, zero-field phase diagram for the $3N$ model in the parameter space. AF, F, H_1, and H_2 mean antiferromagnetic, ferromagnetic, helix 1, and helix 2 configurations, respectively. The straight lines correspond to constant $\mathbf{Q}=\mathbf{G}/p$ commensurate configurations and are shown only for $p \leq 6$. Lines for $p \rightarrow \infty$ (not shown) accumulate at the H-F phase boundary.

phase locking occurs for $p=4$, but the commensurate phase that is locked is not a simple helix. Moreover, we have shown that the helices corresponding to $p=5$ and 6 are certainly locked by the external magnetic field at zero temperature. We think that this is the case for a generic p, even if accidental vanishing of the commensuration energy cannot be excluded *a priori*.

We expect that at a fixed low temperature and low field, the phase diagram in the space of two competing exchange interactions consists of striped regions corresponding to commensurate phases, in between which distorted incommensurate helices are still present. Such a phase diagram is an incomplete devil's staircase generalized to the case of the m-dimensional space of the exchange constants $J_1, J_2, \ldots, J_m$, where J_k is the exchange interaction between kth-nearest neighbors. As the field is increased, the low-order commensurate phases are expected to grow and eventually merge into a complete devil's staircase.

Although a nonzero commensuration energy was not considered in the early works[1,2] for spin models with continuous rotation symmetry, the existence of this phenomenon in the famous anisotropic next-nearest-neighbor Ising (ANNNI) model introduced by Elliott[7] was demonstrated by the definitive analysis of Fisher and Selke.[8] Whereas exchange competition is sufficient to select commensurate configurations in the ANNNI model, this does not happen for models that are invariant under continuous rotation. This different behavior can be understood because the entropy is dependent on the phase of the order-parameter modulation for the Ising model, whereas this is not true for planar XY and Heisenberg models. However, an external magnetic field affects the magnitude of the magnetic moment, giving possible locking as in the ANNNI model. It is intuitively clear that one has phase locking for a longitudinal wave on a discrete lattice, whereas the energy of a transverse wave in a rotationally invariant system must be independent of the phase of the helix. Of course, a field applied in the easy plane induces an amplitude modulation which takes the helical system into the same universality class as the ANNNI model, provided the wave vector is sufficiently close to a rational value.

Another closely related model is the Frenkel-Kontorova (FK) model, which has been the object of detailed mathematical analysis.[9] The Hamiltonian of Eq. (1.1) may be viewed as a generalization of the FK model in the sense that the spatial dependence of ϕ is caused by competing interactions in Eq. (1.1), whereas in the usual versions of the FK model the spatial dependence of ϕ (or the displacement in the model of balls and springs) is due to a suitable harmonic potential involving only nearest-neighbor atoms. If we ignore this difference, then the conclusions of the analysis for the FK model when applied to Eq. (1.1) are as follows. For almost all values of the J_{ij}'s, there exists a critical value H^* of the coupling constant for the periodic potential H. For H less than this critical value, the ground-state configuration is incommensurate and the phase of the helical ground-state configuration can be varied at no cost in energy. (This is the so-called phason degree of freedom.) For H greater than the critical value, the ground state is commensurate and is locked: Varying the phase of the helix requires a definite nonzero energy. For our purposes the main conclusion is that associated with each commensurate state of wavelength pa, where a is a unit of length in the lattice and p is an integer, there is a pinning energy causing the commensurate state to exist over a finite range of J_{ij}'s in parameter space. Thus, as a function of J_{ij}, the wave vector of the helix is described by a devil's staircase, which for small H is incomplete. This behavior of the FK model is thus analogous to that one can argue from Fig. 1 for the planar model. However, note that we find zero pinning energy at zero temperature for $p=3$, in contrast with the result obtained for the FK model.[10]

The FK model[9] is equivalent to the chiral planar model analyzed by Yokoi, Tang, and Chou,[11] at least in the continuum limit. In this model only nearest-neighbor spins are coupled, but this coupling reaches its minimum energy when the NN spins form an angle determined by the chirality parameter. Note that in the model of Yokoi, Tang, and Chou,[11] clockwise and counterclockwise helices correspond to different energies. Although the model of Yokoi, Tang, and Chou allows helical configurations, it is not clear whether real spin systems should be described by this model. If one accounts for the exchange interaction, further couplings in addition to the NN interaction have to be taken into account, so that the direct mapping of the spin model into the FK model is lost.

Briefly, this paper is organized as follows. In Sec. II we describe the perturbation theory in powers of k_BT/J, which we use throughout the paper. In Secs. III, IV, and V we apply this formalism to calculate the commensuration potential for helices in which the wavelength is, respectively, two, three, and four lattice constants. In Sec. VI we present some numerical results for helices of wavelengths five and six lattice constants. On the basis of all our results, we indicate the general form to be expected for the commensuration potential. In Sec. VII we discuss how these results apply to particular models for helimagnets, and in Sec. VIII we summarize our conclusions.

II. LOW-FIELD, LOW-TEMPERATURE PERTURBATION EXPANSION

In this section we carry out a systematic perturbation expansion for the free energy in the low-temperature, low-field limit for the classical planar model with competitive exchange interactions which lead to helical spin configurations[12] when the external magnetic field is absent.

The Hamiltonian we consider is

$$\mathcal{H}=\mathcal{H}(0)-H\sum_i X_i \ , \tag{2.1a}$$

where

$$\mathcal{H}(0)=-\sum_{i,j}J_{ij}\cos(\mathbf{Q}\cdot\mathbf{r}_{ij}+\theta_i-\theta_j) \tag{2.1b}$$

and

$$X_i=\cos(\mathbf{Q}\cdot\mathbf{r}_i+\phi+\theta_i) \ . \tag{2.2}$$

The exchange coupling J_{ij} couples the spins localized on the sites i and j of a regular lattice, H is the external magnetic field (in energy units), the localized magnetic moment μ is assumed to be unit, $\mathbf{r}_i$ is the position of site i, $\mathbf{r}_{ij}=\mathbf{r}_i-\mathbf{r}_j$, and θ_i is the fluctuation in angle of the spin at site i away from its orientation in the undistorted helix. The wave vector of the helix, $\mathbf{Q}$, is determined by minimization of the free energy and will therefore be an implicit function of H and T. Note that we allow the helix to have an arbitrary phase ϕ. In order to completely define the phase in Eq. (2.2), we should state that the origin ($\mathbf{r}$) is chosen to be on a lattice site.

The free energy of the model can be written as an expansion in the magnetic field:

$$F(T,H,\phi,\mathbf{Q})=F_0+F_1H+F_2H^2+F_3H^3+F_4H^4+\cdots \ , \tag{2.3}$$

where

$$F_0=-\frac{1}{\beta}\ln\int D\Theta\, e^{-\beta\mathcal{H}(0)} \ , \tag{2.4}$$

$$F_1=-\sum_i\langle X_i\rangle \ , \tag{2.5}$$

$$F_2=-\frac{1}{2!}\beta\sum_{i,j}\langle X_iX_j\rangle_c \ , \tag{2.6}$$

$$F_3=-\frac{1}{3!}\beta^2\sum_{i,j,k}\langle X_iX_jX_k\rangle_c \ , \tag{2.7}$$

$$F_4=-\frac{1}{4!}\beta^3\sum_{i,j,k,l}\langle X_iX_jX_kX_l\rangle_c \ . \tag{2.8}$$

The subscript c means cumulant,[13] $\beta=(k_BT)^{-1}$, and

$$\langle A\rangle=\frac{\int D\Theta e^{-\beta\mathcal{H}(0)}A}{\int D\Theta e^{-\beta\mathcal{H}(0)}} \ , \tag{2.9}$$

where $D\Theta$ indicates an integration over all variables θ_i. In principle, these integrations should be carried over the interval from $-\pi$ to π. However, to obtain the expansion in powers of T, it is permissible to extend the integration to the infinite interval. Because we have introduced a macroscopic variable ϕ to specify the phase, we must limit the $D\Theta$ integration to a sector of fixed ϕ in phase space. We do this by imposing the constraint $\sum_i\theta_i=0$. We should note that in Eq. (2.3) nonzero values of F_n for odd n are only possible if those F_n have the appropriate nontrivial dependence on ϕ, as we show by examples. For given values of H and T, the actual values of $\mathbf{Q}$ and ϕ are determined as those which minimize $F(T,H,\phi,\mathbf{Q})$ in Eq. (2.3).

In order to reduce the statistical averages to Gaussian integrals, we expand the Hamiltonian (2.1b) in powers of the fluctuations θ_i, obtaining

$$\mathcal{H}(0)=E_0+H_0+\sum_{m=3}^{\infty}V_m \ , \tag{2.10}$$

where

$$E_0=-\sum_{i,j} J_{ij}\cos(\mathbf{Q}\cdot\mathbf{r}_{ij})=-NJ(\mathbf{Q}) , \quad (2.11)$$

$$H_0=\tfrac{1}{2}\sum_{i,j} J_{ij}(\theta_i-\theta_j)^2\cos(\mathbf{Q}\cdot\mathbf{r}_{ij}) , \quad (2.12)$$

$$V_3=-\tfrac{1}{6}\sum_{i,j} J_{ij}(\theta_i-\theta_j)^3\sin(\mathbf{Q}\cdot\mathbf{r}_{ij}) , \quad (2.13)$$

$$V_4=-\tfrac{1}{24}\sum_{i,j} J_{ij}(\theta_i-\theta_j)^4\cos(\mathbf{Q}\cdot\mathbf{r}_{ij}) , \quad (2.14)$$

$$V_5=\tfrac{1}{120}\sum_{i,j} J_{ij}(\theta_i-\theta_j)^5\sin(\mathbf{Q}\cdot\mathbf{r}_{ij}) , \quad (2.15)$$

and so on.

Let us define the Fourier transform of the fluctuation θ_i:

$$\theta_\mu=N^{-1/2}\sum_i e^{i\mu\cdot\mathbf{r}_i}\theta_i , \quad (2.16)$$

where N is the total number of sites. Note from Eq. (2.2) that the constraint of fixed ϕ is simply that $\theta_{\mu=0}=0$. Then Eq. (2.12) becomes

$$H_0=\tfrac{1}{2}\sum_{\mu}{}' G^{-1}(\boldsymbol{\mu})\theta_\mu\theta_{-\mu} , \quad (2.17)$$

where the prime indicates that the sum excludes $\boldsymbol{\mu}=0$ and

$$G^{-1}(\boldsymbol{\mu})=2J(\mathbf{Q})-J(\mathbf{Q}+\boldsymbol{\mu})-J(\mathbf{Q}-\boldsymbol{\mu}) . \quad (2.18)$$

Note that $G(\boldsymbol{\mu})$ is the Fourier transform of the "unperturbed propagator" G_{ij}, defined by

$$G_{ij}=\beta\langle\theta_i\theta_j\rangle_0=\frac{1}{N}\sum_{\mu}{}' G(\boldsymbol{\mu})e^{i\mu\cdot\mathbf{r}_{ij}} , \quad (2.19)$$

where $\langle\cdots\rangle_0$ indicates an average with respect to H_0 given by Eq. (2.17).

Thermal averages as (2.9) can be reduced to Gaussian integrals as follows:

$$\langle A\rangle=\frac{\langle Ae^{-\beta V}\rangle_0}{\langle e^{-\beta V}\rangle_0}=\langle Ae^{-\beta V}\rangle_0^c , \quad (2.20)$$

where the superscript c indicates that only contributions connected (with respect to G_{ij}) are to be kept and $V=\sum_m V_m$. We expand X_i in powers of θ_i:

$$X_i=c_i-\theta_i s_i-\tfrac{1}{2}\theta_i^2c_i+\tfrac{1}{6}\theta_i^3s_i+\tfrac{1}{24}\theta_i^4c_i+\cdots , \quad (2.21)$$

where

$$c_i=\cos(\mathbf{Q}\cdot\mathbf{r}_i+\phi) , \quad (2.22)$$

$$s_i=\sin(\mathbf{Q}\cdot\mathbf{r}_i+\phi) . \quad (2.23)$$

The only quantities appearing in statistical average (2.20) are products of θ_i (c_i and s_i being constants) so that any average can be evaluated as the sum over all contractions in which pairs of variables θ_i and θ_j are replaced by the unperturbed propagator G_{ij} defined by Eq. (2.19). In the following we limit ourselves to the nonzero contributions of lowest order in temperature.

III. EVALUATION OF THE SECOND-ORDER CONTRIBUTION F_2

The linear contribution in Eq. (2.3) gives nonzero contribution at zero temperature only for the ferromagnetic configuration so that it is not of interest in our contest.

The coefficient F_2 of the quadratic contribution in the magnetic field to the free-energy (2.3) may be written

$$F_2=-\frac{1}{2!}\beta\sum_{i,j}\langle X_iX_je^{-\beta V}\rangle_0^c . \quad (3.1)$$

At zero temperature F_2 reduces to

$$F_2^{(0)}=-\tfrac{1}{2}\beta\sum_{i,j}s_is_j\langle\theta_i\theta_j\rangle_0 . \quad (3.2)$$

By using Eq. (2.19) and the identity (for $\mathbf{Q}\neq 0$)

$$\sum_j G_{ij}s_j=G(\mathbf{Q})s_i , \quad (3.3)$$

we obtain

$$F_2^{(0)}=-\tfrac{1}{4}N\left[1-\cos(2\phi)\sum_{\mathbf{G}}\delta(2\mathbf{Q}-\mathbf{G})\right]G(\mathbf{Q}) , \quad (3.4)$$

where $\mathbf{G}$ is a reciprocal-lattice vector.[14] It is easy to see that for $\mathbf{Q}=\mathbf{Q}_{\rm AF}=(\pi/a)(1,1)$, i.e., for the antiferromagnetic configuration, $F_2^{(0)}$ is minimized for $\phi=\pi/2$ and that

$$F_2^{(0)}=-\tfrac{1}{4}N[J(\mathbf{Q}_{\rm AF})-J(\mathbf{0})]^{-1} , \quad (3.5)$$

whereas for a generic $\mathbf{Q}$, $F_2^{(0)}$ is independent of ϕ and one obtains

$$F_2^{(0)}=-\tfrac{1}{4}N[2J(\mathbf{Q})-J(2\mathbf{Q})-J(\mathbf{0})]^{-1} . \quad (3.6)$$

These well-known results[1,15] for the susceptibility of an antiferromagnet and of a generic helix show that the "commensurate" antiferromagnetic (AF) configuration is locked in presence of an external magnetic field so that the existence region of the AF configuration is enhanced in the parameter space at the expense of the configurations having $\mathbf{Q}$ near $\mathbf{Q}_{\rm AF}$. Note that the quadratic contribution of the free energy is phase independent for a generic $\mathbf{Q}$, whereas in the AF configuration $\phi=\pi/2$ (spin-flop phase) has to be chosen in order to minimize the free energy. This is the simplest example of locking of commensurate configurations by magnetic field. Alternatively, one can view phase locking as a type of spin flopping involving a unit cell containing several spins.

IV. EVALUATION OF THE THIRD-ORDER CONTRIBUTION F_3

The cubic term in Eq. (2.3) involves much more complicated algebra, but it concerns the first nontrivial commensurate helix. In this section we evaluate the commensuration energy for the 120° helix which vanishes accidentally at zero temperature, whereas it is not zero for any finite temperature. The coefficient F_3 of the cubic contribution to the free energy is

$$F_3=-\tfrac{1}{6}\beta^2\sum_{i,j,k}\langle X_iX_jX_ke^{-\beta V}\rangle_0^c . \quad (4.1)$$

Expanding both the X_i's and the exponential factor in Eq. (4.1), we obtain

$$F_3=-\tfrac{1}{6}(F_3^{(0)}+k_BTF_3^{(1)}+\cdots)\ , \tag{4.2}$$

where

$$F_3^{(0)}=-\tfrac{3}{2}\beta^2\sum_{i,j,k}c_is_js_k\langle\theta_i^2\theta_j\theta_k\rangle_0^c+\beta^3\sum_{i,j,k}s_is_js_k\langle\theta_i\theta_j\theta_kV_3\rangle_0^c \tag{4.3}$$

and

$$F_3^{(1)}=\sum_{m=1}^{10}T_m\ , \tag{4.4}$$

with

$$T_1=-\beta^5\sum_{i,j,k}s_is_js_k\langle\theta_i\theta_j\theta_kV_3V_4\rangle_0^c\ , \tag{4.5}$$

$$T_2=\tfrac{1}{6}\beta^6\sum_{i,j,k}s_is_js_k\langle\theta_i\theta_j\theta_kV_3^3\rangle_0^c\ , \tag{4.6}$$

$$T_3=\beta^4\sum_{i,j,k}s_is_js_k\langle\theta_i\theta_j\theta_kV_5\rangle_0^c\ , \tag{4.7}$$

$$T_4=\tfrac{3}{2}\beta^4\sum_{i,j,k}c_is_js_k\langle\theta_i^2\theta_j\theta_kV_4\rangle_0^c\ , \tag{4.8}$$

$$T_5=-\tfrac{3}{4}\beta^5\sum_{i,j,k}c_is_js_k\langle\theta_i^2\theta_j\theta_kV_3^2\rangle_0^c\ , \tag{4.9}$$

$$T_6=\tfrac{3}{4}\beta^4\sum_{i,j,k}c_ic_js_k\langle\theta_i^2\theta_j^2\theta_kV_3\rangle_0^c\ , \tag{4.10}$$

$$T_7=-\tfrac{1}{8}\beta^3\sum_{i,j,k}c_ic_jc_k\langle\theta_i^2\theta_j^2\theta_k^2\rangle_0^c\ , \tag{4.11}$$

$$T_8=-\tfrac{1}{2}\beta^4\sum_{i,j,k}s_is_js_k\langle\theta_i^3\theta_j\theta_kV_3\rangle_0^c\ , \tag{4.12}$$

$$T_9=\tfrac{1}{2}\beta^3\sum_{i,j,k}c_is_js_k\langle\theta_i^2\theta_j^3\theta_k\rangle_0^c\ , \tag{4.13}$$

$$T_{10}=\tfrac{1}{8}\beta^3\sum_{i,j,k}c_is_js_k\langle\theta_i^4\theta_j\theta_k\rangle_0^c\ . \tag{4.14}$$

The zero-temperature contribution $F_3^{(0)}$ has the structure

$$F_3^{(0)}=A^{(0)}N\cos(3\phi)\sum_{\mathbf{G}}\delta(3\mathbf{Q}-\mathbf{G})\ . \tag{4.15}$$

The form of Eq. (4.15) indicates a commensuration energy proportional to $A^{(0)}$ for the helix characterized by $\mathbf{Q}=\mathbf{G}/3$. In Appendix A we obtain the result

$$A^{(0)}=G(\mathbf{Q})^2\{\tfrac{3}{4}-\tfrac{3}{4}G(\mathbf{Q})[J(\mathbf{Q})-J(\mathbf{0})]\}\ . \tag{4.16}$$

But $A^{(0)}=0$, since for $\mathbf{Q}=\mathbf{G}/3$ one has

$$G(\mathbf{Q})^{-1}=2J(\mathbf{Q})-J(2\mathbf{Q})-J(\mathbf{0})=J(\mathbf{Q})-J(\mathbf{0})\ . \tag{4.17}$$

In contrast, the quadratic term leads to the locking of the AF phase at all temperatures and, in particular, at $T=0$. For the cubic term we have to evaluate the leading temperature-dependent correction $F_3^{(1)}$ in order to check whether the commensurate configuration with $\mathbf{Q}=\mathbf{G}/3$ is locked by the external magnetic field.

To this aim let us consider the T_m given in Eqs. (4.5)–(4.14). We describe the diagrammatic evaluation of these terms in Appendix B. Summing up all these contributions leads to the result

$$F_3=-\tfrac{1}{6}NAk_BT\cos(3\phi)\sum_{\mathbf{G}}\delta(3\mathbf{Q}-\mathbf{G})+O(T^2)\ , \tag{4.18}$$

where

$$A=\sum_{m=1}^{10}A_m=-\tfrac{9}{2}G(\mathbf{Q})^3I(\mathbf{Q}) \tag{4.19}$$

and

$$I(\mathbf{Q})=\frac{1}{N}\sum_{\boldsymbol{\mu}}\frac{[J(\mathbf{Q}+\boldsymbol{\mu})-J(\boldsymbol{\mu})][J(\mathbf{Q}-\boldsymbol{\mu})-J(\boldsymbol{\mu})]}{[2J(\mathbf{Q})-J(\mathbf{Q}+\boldsymbol{\mu})-J(\boldsymbol{\mu})][2J(\mathbf{Q})-J(\mathbf{Q}-\boldsymbol{\mu})-J(\boldsymbol{\mu})]}\ . \tag{4.20}$$

We have evaluated $I(\mathbf{Q})$ for the linear chain (LC), the square lattice (SL), and the tetragonal lattice (TL) in order to assure that the commensuration energy (4.18) is not zero in one, two, and three dimensions. For the LC the exchange couplings we need are $J_1<0$ and $j_2\equiv J_2/J_1=0.5$. This choice, which assures that $Q=2\pi/3$, gives

$$I(2\pi/3)=\frac{1}{\pi}\int_0^{\pi}d\mu\frac{9(\cos\mu+\cos^2\mu-\frac{1}{2})^2-3\sin^2\mu(1-\cos\mu)^2}{(\cos\mu+\cos^2\mu+\frac{5}{2})^2-3\sin^2\mu(1-\cos\mu)^2}=0.228\,72\ . \tag{4.21}$$

For the SL we consider the line in the parameter space $j_3\equiv J_3/J_1=\frac{1}{2}(1+2j_2)$ on which the helix wave vector is $\mathbf{Q}=(2\pi/3,0)$. For this choice we have

$$I(\mathbf{Q})=\frac{1}{\pi^2}\int_0^{\pi}dx\int_0^{\pi}dy\frac{9a^2-3b^2}{c^2-3b^2}\ , \tag{4.22}$$

where

$$a=\cos x+2j_2\cos x\cos y+j_3\cos(2x)\ , \tag{4.23}$$

$$b=\sin x(1+2j_2\cos y-2j_3\cos x)\ , \tag{4.24}$$

$$c=2-\cos x-4\cos y-2j_2(2+\cos x\cos y)+j_3(7-2\cos^2x-8\cos^2y)\ . \tag{4.25}$$

$I(\mathbf{Q})$ is nearly constant (within a few percent) along the line of the parameter space we have considered. For instance, $j_2=-\frac{5}{8}$ and $j_3=-\frac{1}{8}$ give $I(\mathbf{Q})=0.178\,63$.

We have also considered the TL with in plane interactions up to third neighbors and nearest-neighbor interplane interaction $J'>0$ for $j_3=\frac{1}{2}(1+2j_2)$. This choice gives $\mathbf{Q}=(2\pi/3,0,0)$ and

$$I(\mathbf{Q})=\frac{1}{\pi^3}\int_0^\pi dx\int_0^\pi dy\int_0^\pi dz\frac{9a^2-3b^2}{c'^2-3b^2}\ , \tag{4.26}$$

where a and b are still given by Eqs. (4.23) and (4.24),

$$c'=c+4j'(1-\cos z)\ , \tag{4.27}$$

with $j'=J'/J_1$. $I(\mathbf{Q})$ is nearly independent (within a few percent) of the competing in-plane exchange couplings we have considered, whereas it is strongly dependent on j'. For $j_2=-\frac{5}{8}$ and $j_3=-\frac{1}{8}$, we have $I(\mathbf{Q})=0.14500$ and 0.07017 for $j'=0.1$ and 1, respectively. Note that the commensuration energy decreases as the dimensionality of the model increases, but is nonzero at any finite temperature. The sign of $I(\mathbf{Q})$ assures that one spin over three in the magnetic cell is opposite to the field in the minimum-energy configuration as one can see from Eqs. (4.18) and (4.19). An analogous result was obtained by Kawamura for the NN planar triangular antiferromagnet.[16] It is clear that as the magnetic field is increased, either (a) at some critical value of the field there is a first-order transition in which the orientation of the spin opposing the field changes discontinuously, or (b) there is a critical value of the field above which the orientation of the spin opposing the field changes continuously. In scenario (b) the phase where the orientation changes continuously (we call this an intermediate phase) must be distinct from the paramagnetic phase. In scenario (a) the first-order transition can be to either the paramagnetic phase or an intermediate phase distinct from the paramagnetic phase. Although the commensuration energy we evaluated is nonzero, we realize that long-range order (LRO) at finite temperature does not occur for the LC and SL models. The modulation of the free energy in these cases simply indicates the kind of short-range order (SRO).

V. EVALUATION OF THE FOURTH-ORDER CONTRIBUTION F_4

A quite different behavior is found for exchange couplings leading to $\mathbf{Q}=\mathbf{G}/4$. Indeed, we find that the perturbation expansion starting from the helical configuration suffers from a divergence which is the signature of a dramatic change of the equilibrium configuration.

Let us consider the coefficient F_4 of the quartic power of the field in the free-energy expansion (2.3):

$$F_4=-\tfrac{1}{24}\beta^3\sum_{i,j,k,l}s_is_js_ks_l(-\beta\langle\theta_i\theta_j\theta_k\theta_lV_4\rangle_0^c+\tfrac{1}{2}\beta^2\langle\theta_i\theta_j\theta_k\theta_lV_3^2\rangle_0^c)+\tfrac{1}{12}\beta^4\sum_{i,j,k,l}c_is_js_ks_l\langle\theta_i^2\theta_j\theta_k\theta_lV_3\rangle_0^c$$
$$+\tfrac{1}{36}\beta^3\sum_{i,j,k,l}s_is_js_ks_l\langle\theta_i^3\theta_j\theta_k\theta_l\rangle_0^c-\tfrac{1}{16}\beta^3\sum_{i,j,k,l}c_ic_js_ks_l\langle\theta_i^2\theta_j^2\theta_k\theta_l\rangle_0^c\ . \tag{5.1}$$

Tedious but direct calculations lead to the result, for $T=0$,

$$F_4=NC_0+NC_4\cos(4\phi)\sum_{\mathbf{G}}\delta(4\mathbf{Q}-\mathbf{G})\ , \tag{5.2}$$

where

$$C_0=\tfrac{1}{64}G^4(\mathbf{Q})\{J(\mathbf{Q})-J(3\mathbf{Q})+4G^{-1}(\mathbf{Q})$$
$$-16G(2\mathbf{Q})[J(2\mathbf{Q})-J(\mathbf{Q})]^2\}\ , \tag{5.3}$$

$$C_4=\tfrac{1}{4}G^4(\mathbf{Q})G(2\mathbf{Q})[J(2\mathbf{Q})-J(\mathbf{Q})]^2\ . \tag{5.4}$$

The first term in C_0 is analytic, whereas the second term in C_0 and C_4 are *nonanalytic* because of the presence of the factor

$$G(2\mathbf{Q})=[J(\mathbf{Q})-J(3\mathbf{Q})]^{-1}\ , \tag{5.5}$$

which diverges for $\mathbf{Q}=\mathbf{G}/4$ because $J(\mathbf{Q})=J(3\mathbf{Q})$. This failure of the expansion of the free energy in powers of the magnetic field was pointed out a long time ago.[1] We are able to explain this failure, showing that the stable configuration is completely different from the helix with $\mathbf{Q}=\mathbf{G}/4$. At vanishing magnetic field the stable configuration is an "up-up-down-down" phase with the spin perpendicular to the direction of the magnetic field. In order to prove the above statement, we consider a SL lattice with competing interactions up to third neighbors with $j_2=-\frac{1}{2}$ and $-\frac{1}{4}<j_3<0$.[17] In absence of magnetic field we find stable configurations characterized by a four-spin cell consisting on two interpenetrating antiferromagnetic sublattices, the angle θ between them being arbitrary. Obviously, the angle ϕ that the first spin makes with a reference direction is also arbitrary. We have found that an external magnetic field lifts this double infinite degeneration, because the minimum-energy configuration is given by

$$\cos\phi_1=\cos\phi_2=-\frac{h}{4j_3}\ ,\quad \phi_3=-\phi_2,\quad \phi_4=-\phi_1\ , \tag{5.6}$$

where $h=H/2J_1$ and $\phi_1,\phi_2,\phi_3,\phi_4$ are the angles between the four spins of the magnetic cell and the external magnetic field. This "fan" configuration changes continuously as h increases. For $h\geq h_c=-4j_3$ the spins are saturated in the direction of the field. It is clear that no helix phase exists for any h so that no helix-fan transition occurs in this case. This fact shows that the customary expectation[1] of such a first-order phase transition is not assured for generic exchange competition.

VI. HIGHER-ORDER COMMENSURATE PHASE

In this section we discuss the numerical evaluation of the phase-locking energy for higher-order wave vectors for classical spins at zero temperature. In particular, we focus on the case where $\mathbf{Q}=\mathbf{G}/5$ and $\mathbf{Q}=\mathbf{G}/6$. To treat this case it suffices to consider a linear chain of N spins with nearest- and next-nearest-neighbor interactions.

In the absence of a field, the ground-state energy E_G is

$$e_G=E_G/2J_1N=-\cos Q-j_2\cos(2Q)\ . \qquad (6.1)$$

We want this energy to be minimal when $Q=2\pi/5$, and so

$$0=\frac{de_G}{dQ}=\sin Q+4j_2\sin(2Q)\ . \qquad (6.2)$$

This gives

$$j_2=-\frac{1}{4\cos(2\pi/5)}=-0.809\,02\ . \qquad (6.3)$$

For a fixed wave vector Q, we expect the energy to be of the form

$$e(h)=e_G-\tfrac{1}{2}\chi h^2+O(h^4)-A_5h^5\cos(5\phi)\ , \qquad (6.4)$$

where $h=H/2J_1$,

$$\chi=J_1G(\mathbf{Q})\ , \qquad (6.5)$$

and $G(\mathbf{Q})$ is given by Eq. (2.18). The constant A_5 is the main object of this numerical work: The analogous constant for $\mathbf{Q}=\mathbf{G}/3$ has been shown to vanish for classical spins at zero temperature. We undertook the numerical study of A_5 because the analytic expression for it is extremely complicated.

To study the ground state of the system in question, we kept Q fixed; i.e., we described the ith spin by the angle ϕ_i that it forms with the magnetic field. We require

$$\phi_{i+5}=\phi_i\ . \qquad (6.6)$$

We define the phase ϕ of a periodic configuration by

$$\sum_{i=1}^{5}\phi_i=5\phi+4\pi\ . \qquad (6.7)$$

We start the system from an initial configuration in which

$$\phi_i=(i-1)\frac{2\pi}{5}+\phi,\quad i=1,2,3,4,5\ , \qquad (6.8)$$

and determine the minimum energy for the fixed values of ϕ and h by a relaxation process in which the sum in (6.6), i.e., ϕ, is held constant. The convergence of this scheme was always quite rapid.

We carried out this numerical work for values of h, 0.01, 0.02, and 0.03, and for values of ϕ (in degrees), 0, 12, 18, 24, 36, 48, 54, 60, 72, and 90. The resulting numerical values of the ground-state energy could be fit to the expression in Eq. (6.4) to extremely high precision with the values

$$e_G=-0.963\,525\,4\ , \qquad (6.9)$$

$$\chi=0.178\,885\,4\ , \qquad (6.10)$$

$$A_5=0.003\,704\,1\ . \qquad (6.11)$$

The value of χ we found agrees with the analytic result given in Eq. (6.5). Within the numerical accuracy of double precision, we verified the functional h dependence assumed in Eq. (6.4). Also, there was not the slightest hint of a dependence on ϕ other than that given by $\cos(5\phi)$ as written in Eq. (6.4). So our conclusion is completely unambiguous: The pinning energy A_5 is nonzero even at zero temperature.

We have found that the pinning exists also for $p=6$. In order to have the minimum of e_G given by (6.1) when $Q=\pi/3$, one has to choose $j_2=-0.5$. The expected form for the energy is

$$e(h)=e_G-\tfrac{1}{2}\chi h^2+O(h^4)+A_6h^6\cos(6\phi)\ . \qquad (6.12)$$

Through direct extension to $p=6$ of the analysis performed for $p=5$, we have verified that

$$e_G=-\tfrac{3}{4}\ , \qquad (6.13)$$

$$\chi=\tfrac{2}{5}\ , \qquad (6.14)$$

$$A_6=0.013\,05\ . \qquad (6.15)$$

We consider the cases $p=5$ and 6 as well representative of generic odd and even number of spins per cell. Consequently, one should view the vanishing of A_3 at zero temperature as an accidental peculiarity of that special wave vector. It is interesting that the pinning energy for $p=5$ chooses $\phi=0$, so that one spin in the cell is forced along the field. (When one spin lies along the field, one cannot argue, as we did for the $p=3$ case at the end of Sec. IV, that there *must* be an intermediate phase.) On the contrary, $\phi=\pi/6$ is selected for $p=6$, which allows a symmetric configuration of the spins with respect to the field. We think that the symmetric configurations one finds for $p=5$ and 6 should be intended as models for a generic odd and even value of p, respectively.

VII. LOCKED COMMENSURATE PHASES IN THE 3*N* MODEL

In this section we try to gain some insight about the effect of an in-plane magnetic field on the so called 3*N* model,[17] which consists on a SL of two-dimensional unit spins with competing interactions up to third neighbors, the NN interaction being ferromagnetic. The zero-temperature zero-field phase diagram in the j_2j_3 plane is shown in Fig. 1, where F, AF, H_1, and H_2 regions correspond to ferromagnetic, antiferromagnetic, and two different helical phases, respectively. H_1 is characterized by a wave vector $\mathbf{Q}$ along the (1,0) direction, while the wave vector of H_2 lies along the (1,1) direction. The H_1-H_2 phase boundary $j_2=2j_3$ is an infinite degeneration line[18] because infinite isoenergetic helices minimize the energy of the model. The wave vectors of this degenerate helix (DH) are given by

$$\cos Q_x+\cos Q_y=-\frac{1}{4j_3}\ . \qquad (7.1)$$

The switching of an in-plane external magnetic field H causes the locking of commensurate helices on stripes of width proportional to $h^{p/2}$, where $h=H/2J_1$ and p is the

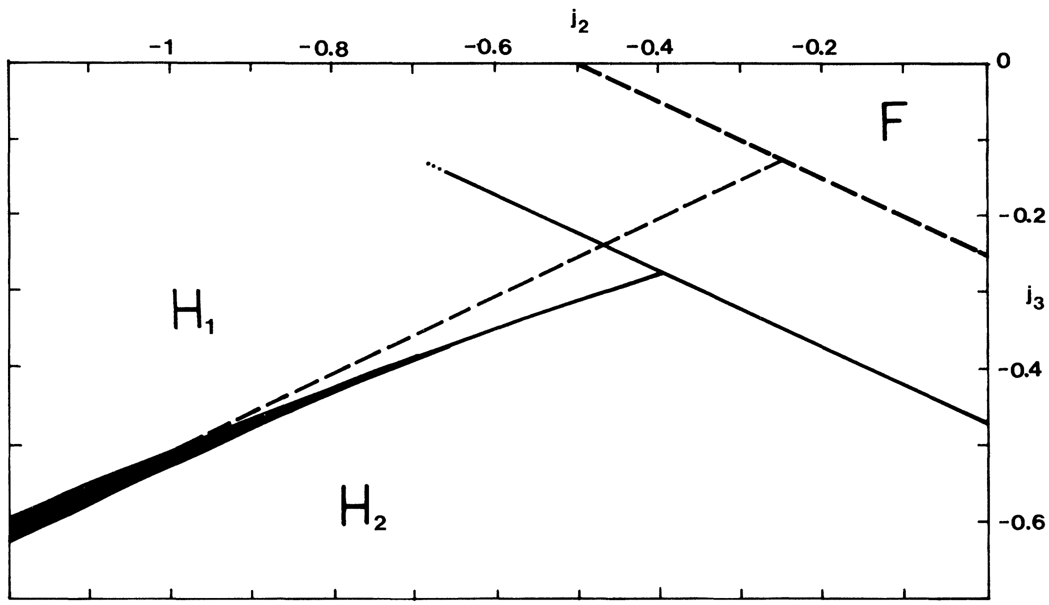

FIG. 2. Projection on the plane j_2, j_3 of the SH existence region for $h = 0.2$ at zero temperature. F, H_1, and H_2 mean ferromagnetic, helix 1, and helix 2 configurations, respectively. The SH phase is stable inside the wedge-shaped shaded area for $j_3 < j_3^* = -0.390\,39$. Dashed lines are the boundary lines at zero magnetic field.

number of spins per cell. For small h the wave vector **Q** shows an incomplete devil's staircase behavior, but for fields strong enough, the devil's staircase is expected to become complete because the commensurate helices cover the whole H_1 and H_2 regions. Obviously, the stripes corresponding to small p are wide, whereas large p have narrow existence regions. We should note that within our formulation it would appear that the transition between the commensurate state and adjacent incommensurate state is a first-order one. However, if one allows for a dilute gas of discommensurations, one sees that this transition is actually continuous. Since we are mainly interested in whether or not the commensuration energy is nonzero, we will not pursue this point further here.

Let us consider the effect of h on the H_1-H_2 phase boundary. It is possible to understand in a systematic way the effect of the magnetic field within h^2 contributions. We have compared the energies of the H_1, H_2, and DH phases that at zero field degenerate on the line $j_2 = 2j_3$. The degeneration line is destroyed by the h^2 contribution, and we have a first-order H_1-H_2 phase transition for $j_3 > j_3^* = -0.390\,39$. For $j_3 < j_3^*$ a "swinging" helix (SH) appears where the helix wave vector changes continuously its direction. This scenario is similar to that one finds in presence of further exchange interactions between more distant spins.[19,20] The SH phase supported by the h^2 contributions exists for $j_3 < j_3^*$ within the region defined by

$$j_2 = 2j_3 + \lambda h^2 , \tag{7.2}$$

where

$$\lambda = -\frac{a j_3}{(1+8j_3)^2 + a^2} , \tag{7.3}$$

with

$$a = \frac{8j_3+1}{4j_3}[2(2j_3+1) - \xi(8j_3+1)], \quad 0 < \xi < 1 . \tag{7.4}$$

The SH wave vector is given by

$$Q_x^{\rm SH} = \cos^{-1}\left[\frac{-1+(1+8j_3)\sqrt{1-\xi}}{8j_3}\right] ,$$
$$Q_y^{\rm SH} = \cos^{-1}\left[\frac{-1-(1+8j_3)\sqrt{1-\xi}}{8j_3}\right] . \tag{7.5}$$

When ξ runs in the range (0,1), j_2 spans the region where SH is defined.

The reduced energy of the SH phase $e_{\rm SH} = E_G / 4J_1 N$ is

$$e_{\rm SH} = \frac{1+16j_3^2}{16j_3} + \left[\frac{16j_3 - 2j_3(1-a) - 1}{512 j_3^2}\lambda + \frac{j_3}{(1+8j_3)^2 + a^2}\right] h^2 . \tag{7.6}$$

Equation (7.6) is directly obtained from Eq. (3.6). The comparison of $e_{\rm SH}$ with the reduced energies e_{H_1} and e_{H_2} for the H_1 and H_2 phases shows that the H_1-SH phase transition is continuous, while the SH-H_2 phase transition is discontinuous. This scenario appears for $j_3 < j_3^*$, whereas for $j_3 > j_3^*$ the SH phase is unstable with respect to the H_1 and H_2 phases. In Fig. 2 we show the phase diagram for $h=0.2$, which corresponds to a magnetic field $H \simeq 11$ T for a typical value of $2J_1 \simeq 20$ K.

We consider now the effect of higher-order contributions in h that favor commensurate configurations. The first-order piece of the H_1-H_2 phase transition is changed into a "scalloplike" profile because the locked commensurate H_1 and H_2 configurations are stable with respect to the incommensurate ones so that they overflow beyond the H_1-H_2 phase boundary obtained within h^2 contributions. For $j_3 < j_3^*$ the wedge-shaped region of the SH phase undergoes analogous modifications in the neighborhood of its boundary lines. Moreover, inside the wedge, "blobs" of locked phases appear in correspondence to commensurate wave vectors in directions other than (1,0) and (1,1).

VIII. SUMMARY AND CONCLUSIONS

We have studied the influence of an external magnetic field on helical configurations of spin models with continuous symmetry. In particular, we have considered the planar model with competing interactions when the field lies in the plane of the spins. The phenomenology of this model is representative also for the classical Heisenberg model with planar anisotropy. Our approach is based on a low-field, low-temperature systematic expansion of the free energy. Note that the problem was already studied by Nagamiya, Nagata, and Kitano[1] on the basis of a variational technique to obtain the minimum-energy configuration of the planar model in presence of an in-plane magnetic field. This calculation brought to the conclusion that helical order is continuously distorted in the range of weak field. Actually, we find that the scenario is somewhat more complex. The calculation of Nagamiya, Nagata, and Kitano indeed concerned only regular contributions in the field, whereas we find additional δ-like contributions that support commensurate configurations. We find that these singular contributions lock the phases corresponding to a generic commensurate value of the helix wave vector both at zero and finite temperature, but the values $\mathbf{Q}=\mathbf{G}/3$ and $\mathbf{Q}=\mathbf{G}/4$ are anomalous. For $\mathbf{Q}=\mathbf{G}/3$, indeed, the commensuration energy vanishes at zero temperature, and for $\mathbf{Q}=\mathbf{G}/4$ we find that the helix configuration is unstable with respect to the onset of an up-up-down-down configuration with the spins nearly perpendicular to the field, analogously to the well known spin-flop phase of a two-sublattice antiferromagnet. Note that the locking of commensurate helices does not correspond strictly to the values of the exchange parameters which give the commensurate helix wave vectors in zero magnetic field. It is easy to see that $\mathbf{Q}$ is affected by contributions of order h^2, so that $\mathbf{Q}$ changes before higher-order singular contributions lock commensurate configurations. In any case the commensuration energy assures a finite range of stability for commensurate helices even if these stability regions do not meet the commensuration lines at zero magnetic field in the parameter space. We mean that zero-field commensurate helices become incommensurate for vanishing magnetic field because the helix distortion prevails on higher-order commensuration effects, but at the same time zero-field incommensurate helices are driven toward commensurate configurations for which the pinning energy will be effective. More precisely, all helices with a $\mathbf{Q}$ wave vector, which at finite magnetic field differs from a commensurate value within $h^{p/2}$, are locked at that commensurate value.

On the basis of our results, an incomplete-devil's-staircase behavior of the helix wave vector through the parameter space is expected for weak magnetic field, while a complete-devil's-staircase behavior could appear for intermediate magnetic field. The former scenario was found for suitable value of the exchange competition in the ANNNI model[8] at zero magnetic field. The phase diagram we find is also similar to that of the FK model.[9] The origin of this similarity is certainly the simultaneous presence of two interaction mechanisms which favor configurations of different periodicity. However, the FK model maps into the model of Yokoi, Tang, and Chou[11] at least in the continuum limit, whereas no formal equivalence between the FK and planar models can be found. We recall that the model of Yokoi, Tang, and Chou[11] is a spin model with interaction restricted to nearest neighbors where helical configurations are introduced by the chiral interaction considered by the authors.

In conclusion, we have shown that locking of commensurate configurations is produced by an external in-plane magnetic field applied to planar spin model with competitive exchange interactions causing helical order in absence of magnetic field. The perturbation approach is given in Sec. II, while Secs. III, IV, V, and VI are devoted to $\mathbf{Q}=\mathbf{G}/2$, $\mathbf{Q}=\mathbf{G}/3$, $\mathbf{Q}=\mathbf{G}/4$, $\mathbf{Q}=\mathbf{G}/5$, and $\mathbf{Q}=\mathbf{G}/6$, respectively. Section VII considers the phenomenology of the so called $3N$ model[17] in the presence of a magnetic field. In Appendixes A and B we give technical details of the diagram expansion for $\mathbf{Q}=\mathbf{G}/3$ at zero and finite temperature, respectively.

ACKNOWLEDGMENTS

This work was supported in part by the National Research Council (CNR) bilateral project Grant No. 88.01738.02 and by the Ministry of Education (MPI). Work at the University of Pennsylvania was supported in part by the National Science Foundation under Grant Nos. DMR 85-19509 and DMR 88-15469. We thank T. C. Lubensky for helpful discussions concerning the FK model.

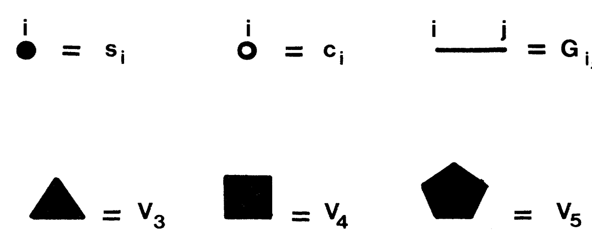

FIG. 3. Basic elements of the low-temperature perturbation expansion. The quantities represented diagrammatically here are given explicitly in Eqs. (A2)–(A7).

FIG. 4. Graphical representation of the two terms written in Eq. (A8).

APPENDIX A: EVALUATION OF $F_3^{(0)}$

In this appendix we give the diagrammatic rules to write the zero-temperature contribution $F_3^{(0)}$ [Eq. (4.3)] to the free-energy expansion

$$F_3^{(0)} = -\tfrac{3}{2}\beta^2 \sum_{i,j,k} c_i s_j s_k \langle \theta_i^2 \theta_j \theta_k \rangle_0^c + \beta^3 \sum_{i,j,k} s_i s_j s_k \langle \theta_i \theta_j \theta_k V_3 \rangle_0^c \ , \quad \text{(A1)}$$

where

$$c_i = \cos(\mathbf{Q}\cdot\mathbf{r}_i + \phi) \ , \quad \text{(A2)}$$

$$s_i = \sin(\mathbf{Q}\cdot\mathbf{r}_i + \phi) \ . \quad \text{(A3)}$$

We recall that

$$\langle \theta_l \theta_m \rangle_0 \equiv k_B T G_{lm} \ . \quad \text{(A4)}$$

We draw the basic components of the perturbation expansion in Fig. 3. The perturbation potentials appearing there are

$$V_3 = -\tfrac{1}{6} J_{lm} \sin(\mathbf{Q}\cdot\mathbf{r}_{lm}) \ , \quad \text{(A5)}$$

$$V_4 = -\tfrac{1}{24} J_{lm} \cos(\mathbf{Q}\cdot\mathbf{r}_{lm}) \ , \quad \text{(A6)}$$

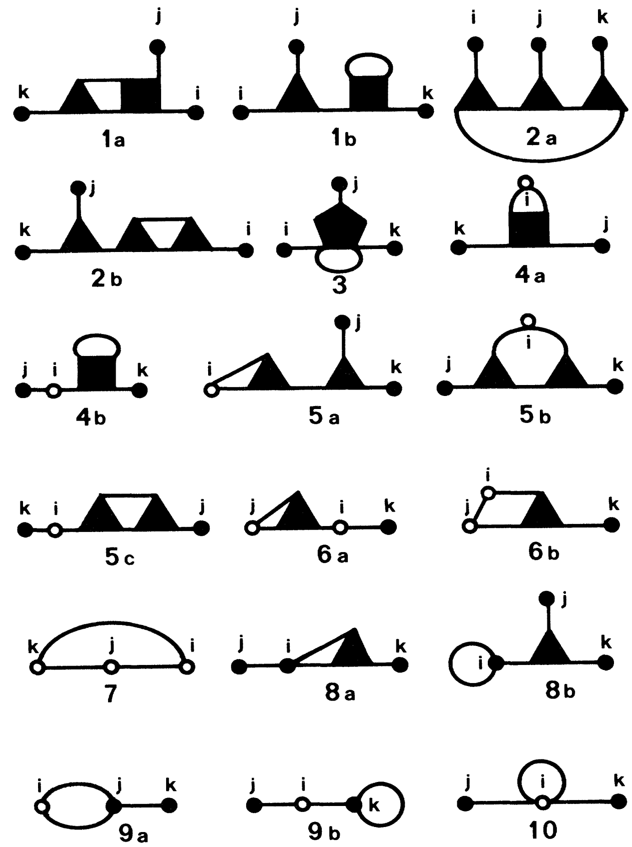

FIG. 5. Graphical development of Eqs. (4.5)–(4.14), which results in the explicit expressions written in Eqs. (B1)–(B10).

$$V_5 = \tfrac{1}{120} J_{lm} \sin(\mathbf{Q}\cdot\mathbf{r}_{lm}) \ . \quad \text{(A7)}$$

There are two equivalent ways to contract the first term of Eq. (A1) in a connected way and six equivalent ways for the second term, and so

$$F_3^{(0)} = -\tfrac{3}{2} \sum_{i,j,k} c_i s_j s_k 2 G_{ij} G_{ik} - \tfrac{1}{6} \sum_{i,j,k,l,m} J_{lm} \sin(\mathbf{Q}\cdot\mathbf{r}_{lm}) s_i s_j s_k 6 (G_{li} - G_{mi})(G_{lj} - G_{mj})(G_{lk} - G_{mk}) \ . \quad \text{(A8)}$$

The graphical representations of the two terms in Eq. (A8) are shown in Fig. 4 by the diagrams 1 and 2, respectively. Using Eq. (3.3), we have

$$F_3^0 = -3G(\mathbf{Q})^2 \sum_i c_i s_i^2 - G(\mathbf{Q})^3 \sum_{l,m} J_{lm} \sin(\mathbf{Q}\cdot\mathbf{r}_{lm})(s_l - s_m)^3 \ . \quad \text{(A9)}$$

In the second term replace l by i and set $\mathbf{r}_m = \mathbf{r}_i + \boldsymbol{\delta}$ and sum over i and $\boldsymbol{\delta}$:

$$F_3^{(0)} = G(\mathbf{Q})^2 \sum_i \left[-3 c_i s_i^2 + G(\mathbf{Q}) \sum_{\delta} J_{\delta} \sin(\mathbf{Q}\cdot\boldsymbol{\delta})(s_i - s_{i+\delta})^3 \right] . \quad \text{(A10)}$$

Disregarding the collinear ferromagnetic configuration ($\mathbf{Q}=\mathbf{G}$), we have

$$\sum_i c_i s_i^2 = -\tfrac{1}{4} N \cos(3\phi) \sum_{\mathbf{G}} \delta(3\mathbf{Q} - \mathbf{G}) \ , \quad \text{(A11)}$$

$$\sum_i \sum_\delta J_\delta \sin(\mathbf{Q}\cdot\boldsymbol{\delta})(s_i - s_{i+\delta})^3 = \tfrac{3}{4}N\cos(3\phi)\sum_{\mathbf{G}} \delta(3\mathbf{Q}-\mathbf{G})[J(\mathbf{0})-J(\mathbf{Q})] \ . \tag{A12}$$

In order to obtain Eq. (A12), we have replaced $J(2\mathbf{Q})$ by $J(-\mathbf{Q})=J(\mathbf{Q})$, $J(3\mathbf{Q})$ by $J(\mathbf{0})$, and $J(4\mathbf{Q})$ by $J(\mathbf{Q})$ because of the δ factor, which forces $3\mathbf{Q}$ to be a reciprocal lattice vector. So doing, we find $F_3^{(0)}$ to be of the form of Eq. (4.15) with $A^{(0)}$ given by Eq. (4.16).

APPENDIX B: EVALUATION OF $F_3^{(1)}$

In this appendix we give the diagrammatic expansions for the temperature-dependent term $F_3^{(1)}$ of Eq. (4.4). We use the diagrammatic formulation discussed in Appendix A involving the diagrammatic elements shown in Fig. 3. In particular, we give the explicit expressions for all T_m given by Eqs. (4.5)–(4.14) and will relate these expressions to the corresponding diagrams which are shown in Fig. 5.

The only nonequivalent ways of contracting T_1 correspond to diagrams 1a and 1b (of Fig. 5) and lead to the result

$$\begin{aligned} T_1 = -\tfrac{1}{144} \sum_{i,j,k,l,m,s,t} & s_i s_j s_k J_{lm} J_{st} \sin(\mathbf{Q}\cdot\mathbf{r}_{lm})\cos(\mathbf{Q}\cdot\mathbf{r}_{st}) \\ & \times[216(G_{is}-G_{it})(G_{js}-G_{jt})(G_{kl}-G_{km})(G_{ls}-G_{ms}-G_{lt}+G_{mt})^2 \\ & +216(G_{il}-G_{im})(G_{jl}-G_{jm})(G_{ks}-G_{kt})(G_{ls}-G_{ms}-G_{lt}+G_{mt})(2G_{ss}-2G_{st})] \ , \end{aligned} \tag{B1}$$

where we used $G_{ss}=G_{tt}$ and $G_{st}=G_{ts}$. For T_2 one has

$$\begin{aligned} T_2 = -\tfrac{1}{1296} \sum_{i,j,k,l,m,q,r,s,t} & s_i s_j s_k J_{lm} J_{qr} J_{st} \sin(\mathbf{Q}\cdot\mathbf{r}_{lm})\sin(\mathbf{Q}\cdot\mathbf{r}_{qr})\sin(\mathbf{Q}\cdot\mathbf{r}_{st}) \\ & \times[1296(G_{iq}-G_{ir})(G_{js}-G_{jt})(G_{kl}-G_{km})(G_{ls}-G_{lt}-G_{ms}+G_{mt}) \\ & \times(G_{lq}-G_{lr}-G_{mq}+G_{mr})(G_{qs}-G_{qt}-G_{rs}+G_{rt})+1944(G_{iq}-G_{ir})(G_{jl}-G_{jm}) \\ & \times(G_{kl}-G_{km})(G_{ls}-G_{lt}-G_{ms}+G_{mt})(G_{qs}-G_{qt}-G_{rs}+G_{rt})^2] \ . \end{aligned} \tag{B2}$$

The corresponding diagrams are 2a and 2b. Next we consider T_3. Corresponding to diagram 3, we have

$$T_3 = \tfrac{1}{120} \sum_{i,j,k,l,m} s_i s_j s_k J_{lm} \sin(\mathbf{Q}\cdot\mathbf{r}_{lm}) 60(G_{il}-G_{im})(G_{jl}-G_{jm})(G_{kl}-G_{km})(2G_{ll}-2G_{lm}) \ . \tag{B3}$$

The term T_4, which involves diagrams 4a and 4b is written as

$$\begin{aligned} T_4 = -\tfrac{1}{16} \sum_{i,j,k,l,m} & c_i s_j s_k J_{lm} \cos(\mathbf{Q}\cdot\mathbf{r}_{lm}) \\ & \times[24(G_{il}-G_{im})^2(G_{jl}-G_{jm})(G_{kl}-G_{km})+48G_{ji}(G_{il}-G_{im})(2G_{ll}-2G_{lm})(G_{lk}-G_{mk})] \ . \end{aligned} \tag{B4}$$

For T_5 we have

$$\begin{aligned} T_5 = -\tfrac{1}{48} \sum_{i,j,k,l,m,s,t} & J_{lm} J_{st} \sin(\mathbf{Q}\cdot\mathbf{r}_{lm})\sin(\mathbf{Q}\cdot\mathbf{r}_{st}) c_i s_j s_k \\ & \times[72(G_{il}-G_{im})^2(G_{ls}-G_{ms}-G_{lt}+G_{mt})(G_{js}-G_{jt})(G_{ks}-G_{kt}) \\ & +144(G_{il}-G_{im})(G_{is}-G_{it})(G_{ls}-G_{ms}-G_{lt}+G_{mt})(G_{jl}-G_{jm})(G_{ks}-G_{kt}) \\ & +144G_{ik}(G_{il}-G_{im})(G_{ls}-G_{ms}-G_{lt}+G_{mt})^2(G_{js}-G_{jt})] \ . \end{aligned} \tag{B5}$$

Diagrams referring to T_5 are 5a, 5b, and 5c. We turn to T_6:

$$T_6 = -\tfrac{1}{8} \sum_{i,j,k} c_i c_j s_k J_{lm} \sin(\mathbf{Q}\cdot\mathbf{r}_{lm})[24G_{ik}(G_{il}-G_{im})(G_{jl}-G_{jm})^2+24G_{ij}(G_{kl}-G_{km})(G_{il}-G_{im})(G_{jl}-G_{jm})] \ . \tag{B6}$$

The diagram representation of Eq. (B6) is given by diagrams 6a and 6b. For T_7 we have the contribution of diagram 7, which gives

$$T_7 = -\tfrac{1}{8} \sum_{i,j,k} c_i c_j c_k 8G_{ij}G_{jk}G_{ki} \ . \tag{B7}$$

We turn next to T_8, which has contributions from diagrams 8a and 8b:

$$T_8 = \tfrac{1}{12} \sum_{i,j,k,l,m} J_{lm} \sin(\mathbf{Q}\cdot\mathbf{r}_{lm}) s_i s_j s_k [36G_{ij}(G_{il}-G_{im})^2(G_{kl}-G_{km})+18G_{ii}(G_{il}-G_{im})(G_{jl}-G_{jm})(G_{kl}-G_{km})] \ . \tag{B8}$$

The term T_9 is represented by diagrams 9a and 9b and is given by

$$T_9=\frac{1}{2}\sum_{i,j,k} c_i s_j s_k(6G_{ij}^2 G_{jk}+6G_{kk}G_{ij}G_{ik}) . \tag{B9}$$

Finally, the term T_{10} is given by diagram 10 as

$$T_{10}=\frac{1}{8}\sum_{i,j,k} c_i s_j s_k 12G_{ii}G_{ij}G_{ik} . \tag{B10}$$

The above terms can be simplified following the approach of Appendix A. Thereby, we find that

$$T_m = A_m N\cos(3\phi)\sum_{\mathbf{G}}\delta(3\mathbf{Q}-\mathbf{G}) , \tag{B11}$$

where

$$A_1=-[G(\mathbf{Q})]^3(1/N)\sum_{\mu} G(\mu)\{\tfrac{3}{8}G(\mathbf{Q}+\mu)[2J(\mathbf{Q}-\mu)-J(\mathbf{Q}+\mu)-J(\mu)-J(\mathbf{Q})+J(0)]^2 + \tfrac{9}{4}[J(\mathbf{Q})-J(0)-\tfrac{1}{2}J(\mathbf{Q}+\mu)-\tfrac{1}{2}J(\mathbf{Q}-\mu)+J(\mu)]\} , \tag{B12}$$

$$A_2=-[G(\mathbf{Q})]^3(1/N)\sum_{\mu} G(\mu)G(\mathbf{Q}+\mu)\{\tfrac{9}{8}[J(0)-J(\mathbf{Q})-J(\mathbf{Q}+\mu)-J(\mu)+2J(\mathbf{Q}-\mu)]^2 - \tfrac{1}{4}G(\mathbf{Q}-\mu)[J(\mathbf{Q})-J(0)+J(\mathbf{Q}-\mu)+J(\mathbf{Q}+\mu)-2J(\mu)] \times[J(\mathbf{Q})-J(0)+J(\mathbf{Q}+\mu)+J(\mu)-2J(\mathbf{Q}-\mu)] \times[J(\mathbf{Q})-J(0)+J(\mathbf{Q}-\mu)+J(\mu)-2J(\mathbf{Q}+\mu)]\} , \tag{B13}$$

$$A_3=-\tfrac{3}{4}[G(\mathbf{Q})]^3(1/N)\sum_{\mu} G(\mu)[J(0)-J(\mathbf{Q})-J(\mu)+J(\mathbf{Q}+\mu)] , \tag{B14}$$

$$A_4=[G(\mathbf{Q})]^2(1/N)\sum_{\mu} G(\mu)\{\tfrac{3}{8}G(\mathbf{Q}-\mu)[J(\mathbf{Q})-J(0)-2J(\mathbf{Q}+\mu)+J(\mu)+J(\mathbf{Q}-\mu)] + \tfrac{3}{2}G(\mathbf{Q})G(\mu)[J(\mathbf{Q})-J(0)-J(\mathbf{Q}+\mu)+J(\mu)]\} , \tag{B15}$$

$$A_5=[G(\mathbf{Q})]^2(1/N)\sum_{\mu} G(\mu)G(\mu-\mathbf{Q})\{\tfrac{9}{8}[J(\mathbf{Q})+J(\mathbf{Q}-\mu)-2J(\mathbf{Q}+\mu)+J(\mu)-J(0)] - \tfrac{3}{4}G(\mathbf{Q}+\mu)[J(0)+2J(\mu)-J(\mathbf{Q})-J(\mathbf{Q}-\mu)-J(\mathbf{Q}+\mu)] \times[2J(\mathbf{Q}+\mu)+J(0)-J(\mathbf{Q}-\mu)-J(\mathbf{Q})-J(\mu)] + \tfrac{3}{4}G(\mathbf{Q})[J(\mathbf{Q})-J(0)+J(\mathbf{Q}-\mu)+J(\mu)-2J(\mathbf{Q}+\mu)]^2\} , \tag{B16}$$

$$A_6=G(\mathbf{Q})(1/N)\sum_{\mu} G(\mu)G(\mathbf{Q}+\mu)\{-\tfrac{3}{4}G(\mathbf{Q})[J(\mathbf{Q})-J(0)+J(\mathbf{Q}+\mu)-2J(\mathbf{Q}-\mu)+J(\mu)] + \tfrac{3}{4}G(\mathbf{Q}-\mu)[J(\mathbf{Q})-J(0)+J(\mathbf{Q}+\mu)+J(\mathbf{Q}-\mu)-2J(\mu)]\} , \tag{B17}$$

$$A_7=(-1/4N)\sum_{\mu} G(\mu)G(\mathbf{Q}+\mu)G(\mathbf{Q}-\mu) , \tag{B18}$$

$$A_8=[G(\mathbf{Q})]^2(1/N)\sum_{\mu} G(\mu)\{\tfrac{9}{8}+\tfrac{3}{4}G(\mathbf{Q}-\mu)[J(\mathbf{Q})+J(\mu)+J(\mathbf{Q}-\mu)-J(0)-2J(\mathbf{Q}+\mu)]\} , \tag{B19}$$

$$A_9=(-3/4N)G(\mathbf{Q})\sum_{\mu} G(\mu)[G(\mu+\mathbf{Q})+G(\mathbf{Q})] , \tag{B20}$$

$$A_{10}=(-3/8N)[G(\mathbf{Q})]^2\sum_{\mu} G(\mu) . \tag{B21}$$

Collecting these results, we obtain Eqs. (4.18)–(4.20) of the text.

[1]T. Nagamiya, K. Nagata, and Y. Kitano, Prog. Theor. Phys. **27**, 1253 (1962).
[2]T. Nagamiya, in *Solid State Physics*, edited by F. Seitz and D. Turnbull (Academic, New York, 1967), Vol. 20, p. 346.
[3]R. J. Elliott and R. V. Lange, Phys. Rev. **152**, 235 (1966).
[4]H. Thomas and P. Wolf, in *Proceedings of the International Conference on Magnetism* (Institute of Physics and the Physical Society, London, 1965), p. 731.
[5]A. B. Harris, E. Rastelli, and A. Tassi, J. Appl. Phys. **67**, 5445 (1990).

[6]A. B. Harris, J. Appl. Phys. **69**, (1991).
[7]R. J. Elliott, Phys. Rev. **124**, 346 (1961).
[8]M. E. Fisher and W. Selke, Phys. Rev. Lett. **44**, 1502 (1980).
[9]See, for instance, P. Bak, Rep. Prog. Phys. **45**, 587 (1982).
[10]G. Theodorou and T. M. Rice, Phys. Rev. B **18**, 2840 (1978).
[11]C. S. Yokoi, L. H. Tang, and W. Chou, Phys. Rev. B **37**, 2173 (1988).
[12]J. Villain, J. Phys. Chem. Solids **11**, 303 (1959); A. Yoshimori, J. Phys. Soc. Jpn. **14**, 807 (1959); T. A. Kaplan, Phys. Rev. **116**, 888 (1959).
[13]See, for instance, S. K. Ma, *Statistical Mechanics* (World Scientific, Philadelphia, 1985), p. 203.
[14]Here and below we encounter the quantity $I_p(\mathbf{Q}) \equiv \sum_{\mathbf{G}} \delta(p\mathbf{Q}-\mathbf{G})$. Here it is understood that $\mathbf{G}$ is summed over values such that $\mathbf{G}/p$ is confined to the first Brillouin zone.
[15]H. Yoshiyama, N. Suzuki, and K. Motizuki, J. Phys. C **17**, 713 (1984).
[16]H. Kawamura, J. Phys. Soc. Jpn. **53**, 2452 (1984).
[17]E. Rastelli, A. Tassi, and L. Reatto, Physica **97B**, 1 (1979).
[18]E. Rastelli, L. Reatto, and A. Tassi, J. Phys. C **16**, L331 (1983).
[19]A. B. Harris, E. Rastelli, and A. Tassi, Solid State Commun. **75**, 35 (1990).
[20]E. Rastelli and A. Tassi, Z. Phys. B **75**, 211 (1989).